Assessing variability in post-fire forest structure along gradients of productivity in the Canadian boreal using multi-source remote sensing

Douglas K. Bolton[1*], Nicholas C. Coops[1], Txomin Hermosilla[1], Michael A. Wulder[2], Joanne C. White[2]

[1]Integrated Remote Sensing Studio, Department of Forest Resources Management, Faculty of Forestry, University of British Columbia, 2424 Main Mall, Vancouver, British Columbia, V6T 1Z4, Canada

[2]Canadian Forest Service (Pacific Forestry Centre), Natural Resources Canada, 506 West Burnside Road, Victoria, British Columbia, V8Z 1M5, Canada

[*]Corresponding author
Tel. 604-822-6592
Email. doug.k.bolton@ubc.ca

Keywords: Disturbance, forest regeneration, boreal forest structure, Landsat, lidar, MODIS, productivity

Pre-print of published version

Reference:
Bolton, D.K., Coops, N.C., Hermosilla, T., Wulder, M.A., White, J. C., 2017. Assessing variability in post-fire forest structure along gradients of productivity in the Canadian boreal using multi-source remote sensing. *Journal of Biogeography.*

DOI:
http://dx.doi.org/10.1111/jbi.12947

Abstract

Aim

Forest regeneration following fire is an important component of the global carbon cycle, but it is difficult to monitor over large and remote forested regions, such as Canada's north. In this study, we aim to 1) characterize how forest regeneration following fire varies across the Canadian boreal and 2) determine if this variability is captured by satellite-derived estimates of productivity.

Location

Canadian boreal

Methods

We relate structural measurements from light detection and ranging (lidar) data to gross primary productivity (GPP) estimates from the MODerate Resolution Imaging Spectroradiometer (MODIS) along a 25-year chronosequence of forest regeneration following fire. Over 400 patches that burned from 1985–2009 were analysed, with fire information obtained from a national Landsat-derived record of forest change.

Results

In the first 15 years since fire (YSF), estimates of percent canopy cover (> 2m) were typically low regardless of GPP (mean = 11.0–16.0%, sd = 7.8-8.9%) and correlations to GPP were relatively weak ($r = 0.18$–0.48). Canopy cover was more variable between stands by 16 – 25 YSF (mean = 16.2 – 21.7%, sd = 16.0–17.1%), and correlations to GPP were stronger ($r = 0.63$-0.71, $p < 0.01$). Conversely, variability in stand height (75th height percentile) remained low at 16 – 25 YSF (mean = 4.9 – 5.0m, sd = 0.9 – 1.1m) and weakly related to GPP ($r = 0.16$ – 0.21).

Main Conclusions

Satellite-derived estimates of productivity capture differences in canopy structure across the boreal, but only after 15 YSF. While canopy cover varied strongly along gradients of productivity from 16 – 25 YSF, differences in vertical growth were less pronounced due to slow boreal growth rates. Our results provide important insights into how satellite-derived estimates of productivity are realized structurally, as understanding regional variation in forest regeneration is critical to quantifying carbon dynamics in forests. Combining lidar-derived estimates of structure with Landsat-derived disturbance history is a valuable approach for characterizing variability in post-fire structure over large forested areas.

1. Introduction

Globally, boreal forests store an estimated 32% of the 861±66 petagrams of the carbon stored in the terrestrial biosphere, and accounted for an estimated 21% of the terrestrial carbon sink between 1990 – 2007 (Pan *et al.*, 2011). Despite playing an important role in the global carbon cycle, spatial and temporal variability in aboveground biomass remains poorly quantified in many boreal regions due to a scarcity of field measurements (Gillis *et al.*, 2005; Kurz *et al.*, 2013). Across the Canadian boreal, for example, roughly 60% of forests are unmanaged (Venier *et al.*, 2014), and therefore not subjected to routine forest inventory (Gillis *et al.*, 2005). Without sufficient field measurements, Canada's unmanaged boreal remains a source of uncertainty in both national (Kurz *et al.*, 2013) and global (Pan *et al.*, 2011) efforts to characterize forest carbon budgets. In order to reduce uncertainties around the amount of carbon stored in aboveground biomass, additional measurements of three-dimensional forest structure are needed across Canada's unmanaged boreal, in addition to an improved characterization of how structure varies through time.

Across Canada's unmanaged boreal, temporal variability in forest structure is driven primarily by natural disturbance and recovery dynamics (Kasischke *et al.*, 1995; Kurz *et al.*, 2013). Stand-replacing disturbances, principally fire, result in large fluxes of carbon from forests to the atmosphere through the combustion of biomass and the decay of dead plant material (Kasischke *et al.*, 1995; Amiro *et al.*, 2001). In the years following a stand-replacing fire, carbon is typically re-sequestered as pioneer trees establish and grow (Johnstone *et al.*, 2004; Kurz *et al.*, 2013). The rate at which carbon is sequestered, referred to here as forest productivity, will dictate how quickly the biomass lost to disturbance is recovered. A quantification of the relationships between fire history, forest productivity, and forest structure, and methods to monitor these relationships over large forested areas, can provide an improved understanding of both spatial and temporal variability in boreal forest structure, which is critical for carbon modelling activities.

While localized studies have provided strong characterizations of the impacts of disturbance and productivity on forest structure (e.g., Boucher *et al.*, 2006; Larson *et al.*, 2008), few studies have attempted to quantify these relationships over large forested regions. In the remote northern boreal of Canada, where inventory and plot data are scarce (Gillis *et al.*, 2005; Kurz *et al.*, 2013), our ability to quantify these relationships with existing field data is limited. Alternatively, remote sensing technologies are capable of detecting forest disturbances (e.g., Huang *et al.*, 2010; Kennedy *et al.*, 2010), monitoring forest productivity (e.g., Hicke *et al.*, 2003; Running *et al.*, 2004), and measuring vegetation structure over large areas (e.g., Bolton *et al.*, 2013; Kane *et al.*, 2014). Landsat imagery, in particular, has been used for decades to detect and describe forest disturbances (Hansen & Loveland, 2012; Wulder *et al.*, 2012a). With the opening of the Landsat archive in 2008 (Wulder *et al.*, 2012a) and advances in data products and processing (Hansen & Loveland, 2012), patterns of forest change can now be studied at regional to national extents using Landsat data. Recently, Hermosilla *et al.* (2016) utilized Landsat imagery to produce annual records of forest disturbance across the forested ecosystems of Canada from 1985 to 2011 at a spatial resolution of 30 m. This dataset provides an unprecedented look at forest change across Canada, and allows the location and spatial extent of recent boreal fires to be accurately assessed.

While disturbances can be detected and described using Landsat time-series data, our ability to assess the impact of fire on structure and subsequent regrowth is limited by a lack of plot- or remote sensing-based information on three-dimensional forest structure (Gillis *et al.*, 2005; Kurz *et al.*, 2013; Bartels *et al.*, 2016). In order to quantify how disturbances impact structure, researchers have used a fusion of Landsat time-series and light detection and ranging (lidar) data (e.g., Lefsky *et al.*, 2005; Kane *et al.*, 2014). By emitting millions of laser pulses over forest canopies, typically from an airborne platform, lidar sensors can produce a three-dimensional cloud of points describing the structure of forest canopies, from which important indictors of carbon storage, such as canopy cover and stand height, can be estimated (Lim *et al.*, 2003). When used in concert, these sources of remotely sensed data provide an opportunity to both detect disturbances as well as quantify their impact on forest structure (Kane *et al.*, 2013, 2014; Bolton *et al.*, 2015).

In 2010, transects of airborne lidar data totaling ~25,000 km in length were collected across the Canadian boreal (Wulder *et al.*, 2012b), providing an opportunity to assess forest structure over large swaths of boreal forests. Magnussen and Wulder (2012) used these data to assess canopy height variation for 163 fires recorded in the Canadian National Fire Database (CNFDB), a collection of historical fire data from management agencies across Canada. As fire perimeters in the CNFDB often contain a mosaic of burned and unburned forest patches, Magnussen and Wulder (2012) required a statistical approach to distinguish young, regenerating canopies from stands that did not burn. To more precisely distinguish fire perimeters, Bolton *et al.* (2015) used Landsat time-series information in place of the CNFDB to detect fires, and assessed post-fire structure along portions of these transects using lidar-derived metrics.

Here, we combine fire disturbances mapped by Hermosilla *et al.* (2016) across the entire Canadian boreal from 1985-2009 with structural metrics along 25,000 km of lidar transects to assess variability in post-fire structure. We characterize how forest regeneration varies along gradients of productivity by relating structural metrics to satellite-derived estimates of gross primary productivity (GPP) from the MODerate Resolution Imaging Spectroradiometer (MODIS). Using these data, we ask the following two questions:

How does variability in stand structure change as a function of time since fire?

As high-intensity crown fires dominate the Canadian boreal, stands typically consist of little to no live tree cover in the first years following fire (Mack *et al.*, 2008; de Groot *et al.*, 2013). Forest regeneration and carbon uptake following fire will vary both locally and regionally due to a multitude of factors, including regeneration method (i.e., vegetative regeneration or from seed), species composition, site conditions, and climate (Johnstone *et al.*, 2004; Kurz *et al.*, 2013; Bartels *et al.*, 2016). Here, we are interested in determining how quickly differences in early stand succession are realized structurally following fire across the boreal. As boreal trees take several years to establish from seed (Johnstone *et al.*, 2004), and growth rates are typically slow (Bonan & Shugart, 1989), we expect variability in structure between stands to be relatively low in the first decade following fire, and increase in the second decade as differences in newly formed canopies become pronounced. Earlier regeneration may be possible on sites dominated by broadleaf species, such as trembling aspen (*Populus tremuloides*) or white birch (*Betula papyrifera*), as these species are capable of sprouting from roots or stumps (i.e., vegetative regeneration) and have faster growth rates than coniferous species (Chen & Popadiouk, 2002; Johnstone *et al.*, 2004; Bartels *et al.*, 2016). While we expect variance in structure to increase during the length of this study (25 years following fire), we would not expect variance to increase indefinitely (Pare & Bergeron, 1995; Harper *et al.*, 2002). For example, high productivity sites colonized by trembling aspen may decrease in height once the initial cohort of trees die and is replaced by late successional conifers (Pare & Bergeron, 1995), reducing the difference in height compared to less productive stands.

Does this variability in stand structure correlate to coarse-resolution satellite-derived estimates of productivity?

Coarse-resolution (1-km) estimates of GPP from MODIS are a valuable source of information for describing regional and landscape-level variability in forest productivity (Running *et al.*, 2004). Here, we are interested in understanding if these estimates of productivity can inform on the variability we observe in early stand structure. In the immediate years following fire, prior to the formation of new canopies, productivity will not likely be an important factor in describing structural variability, as variability will be more a function of fire severity and pre-disturbance structure (Boulanger & Sirois, 2006; Angers *et al.*, 2011). As time since fire increases, differences in structure that are driven by regional variability in productivity will become more pronounced, and the correlation between structural attributes and productivity should increase. However, local variations in fire severity, site conditions, and species composition may leave a large portion of variation in structure unexplained by coarse-resolution productivity estimates.

By addressing these questions, we provide an improved understanding of the influence of both time since fire and forest productivity on boreal forest structure and recovery, and characterize how forest recovery varies spatially across the Canadian boreal.

2. Methods

2.1. *Study area*

The Canadian boreal spans over 550 million ha, of which 270 million ha is treed (Brandt *et al.*, 2013), and is dominated by cold-tolerant coniferous species, such as black spruce (*Picea mariana)*, white spruce (*Picea glauca*), and balsam fir (*Abies balsamea*). Broadleaf species, such as trembling aspen and white birch, are more abundant in the southern boreal as well as on sites with thin organic layers (Ecological Stratification Working Group, 1996).

The majority of the northern boreal is 'de facto' protected, as access to these forests is limited (Andrew *et al.*, 2012), resulting in forested ecosystems that are dominated by natural disturbance and recovery dynamics. Fire frequency generally increases from east to west across the boreal, as conditions in the west are drier and the probability of lightning strikes is higher, with fire frequency varying from several decades to several centuries (Ryan, 2002; Brassard & Chen, 2006). In addition to fire, these northern forests are also altered by insects, disease, and windthrow (Chen & Popadiouk, 2002; Brassard & Chen, 2006). While the northern boreal is de facto protected, southern regions of the boreal are actively managed for timber (Brandt *et al.*, 2013). For this analysis, only forests falling within the Brandt (2009) definition of the boreal were assessed, with the treeline representing the northern extent of the boreal and the boundary with the hemiboreal representing the southern extent, where cold-tolerant boreal species begin to transition to temperate deciduous species.

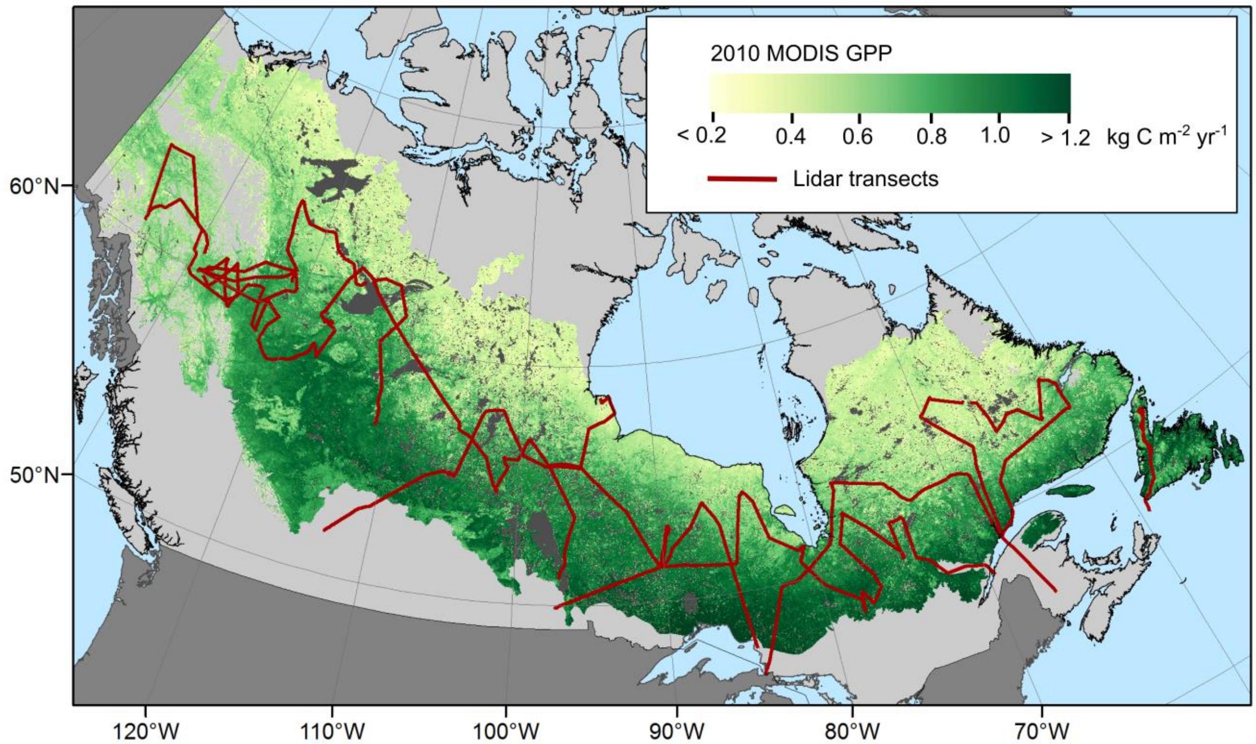

Figure 1: Transects of airborne lidar data collected in 2010 across the Canadian boreal, overlaid on 2010 gross primary productivity (GPP) estimates from MODIS. Estimates of GPP are only shown for cells within the boreal zone defined by Brandt (2009)

2.2. ***Data***

2.2.1. *Lidar structural measurements*

In the summer of 2010, 34 transects of airborne lidar data were collected across the northern boreal of Canada (Fig. 1), from which lidar structural metrics were derived on a 25 m grid (Wulder *et al.*, 2012b, see Appendix S1 for details). From these data, two key indicators of aboveground biomass were assessed: canopy cover and stand height. Canopy cover was calculated as the percentage of first returns intercepted above 2 m to the total number of first returns, in order to relate closely to field definitions of canopy cover (Jennings *et al.*, 1999). Stand height was assessed as the 75th height percentile of first returns. Height percentiles, which represent a direct measure of vertical structure from lidar, correlate strongly to common measures of stand height such as dominant tree height and Lorey's height (Næsset *et al.*, 2004; Wulder *et al.*, 2012b). Upper height percentiles, such as the 95th or 99th, will likely describe the height of residual structures (e.g., snags or surviving trees) in the immediate years following fire, as these upper percentiles inform on the height of the tallest objects in a stand. Alternatively, the 75th height percentile will be more sensitive to vegetation regrowth, and less influenced by several tall residual structures once new canopies begin to form. Therefore, the 75th height percentile was used in this study as a surrogate for dominant tree height. To remove the impact of returns from low vegetation and the ground, only first returns above 2 m were used in the calculation of the 75th height percentile.

2.2.2. *Landsat disturbance detection*

To identify burned patches, we used Landsat-derived disturbance information produced by Hermosilla *et al.* (2016). Following the Composite 2 Change (C2C) approach, Hermosilla *et al.* (2016) detected change events across the entire land base of Canada from 1985 – 2011, with each change event attributed to a change type (Figure 2, see Appendix S1 for details on the C2C approach).

2.2.3. *MODIS Gross Primary Productivity*

MODIS GPP was used as an indicator of landscape productivity following fire. Both 8-day and annual estimates of GPP are available from 2000-2015 as part of NASA's MOD17 product at 1-km spatial resolution (Running *et al.* 2004). To ensure that GPP estimates were representative of post-fire conditions, and corresponded to the timing of the lidar flights, we used estimates of annual GPP from 2010 (see Appendix S1 for details on the MODIS GPP algorithm and preprocessing).

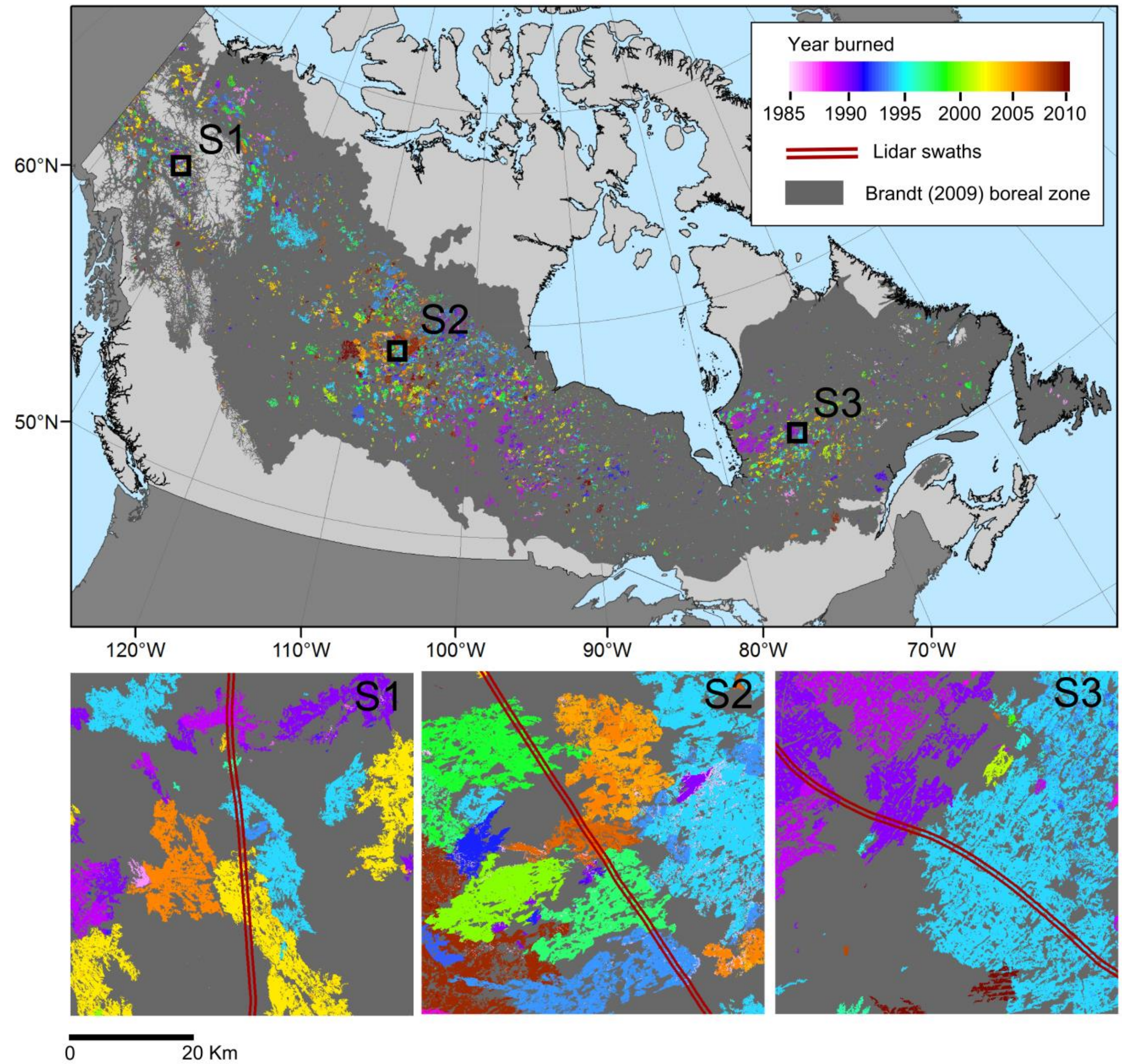

Figure 2: Areas detected as burned (1985–2011) across the Canadian boreal following the Composites 2 Change (C2C) approach. Panels S1, S2, S3 are examples of the intersect between detected fires and lidar transects

2.3. *Selection of lidar cells*

We removed lidar cells classified as water, wetlands, agriculture, and developed areas using information on land cover from the Earth Observation for Sustainable Development of Forests (EOSD) dataset (http://tree.pfc.forestry.ca/). This land cover dataset is a circa 2000 Landsat-derived classification of Canada's forested ecosystems, produced by the Canadian Forest Service, along with federal, provincial, and university partners (see Wulder *et al.*, 2008). To augment the EOSD in the removal of wetlands, areas mapped as inundated in the Global Inundation Extent from Multi-Satellites-15 (GIEMS-15) dataset, a high spatial resolution map of global inundated areas (15 arc-seconds), were also removed (see Fluet-Chouinard *et al.*, 2015). To avoid areas with high anthropogenic impact, lidar cells within 1 km of a road were masked using the 2010 Canadian Road Network File (available at: https://www12.statcan.gc.ca/census-recensement/2011/geo/RNF-FRR/index-eng.cfm).

2.4. *Assessment of post-fire structure*

Lidar-derived estimates of canopy cover and stand height, and estimates of GPP from MODIS, were averaged across each burned patch. The contribution of each 1-km GPP pixel to the patch average was proportional to the area of lidar data that the pixel contained. Only burned patches containing > 5 ha of suitable lidar data were analysed (i.e., lidar cells meeting the criteria in the previous section). If no trees greater than 2 m in height were present in a 25 m lidar cell (i.e., canopy cover = 0%), then that lidar cell did not contribute to the patch average for the 75th height percentile.

Burned patches were split into five groups based on years since fire (1–5, 6–10, 11–15, 16–20, 21–25 years since fire), and the relationship between lidar-derived structural metrics and satellite-derived GPP was assessed within each group using Pearson's correlation coefficient and the modified *t*-test developed by Clifford *et al.* (1989) and altered by Dutilleul (1993) (See Appendix S2 for details on the modified *t*-test).

In total, structure was assessed for 417 patches that burned from 1985 to 2009. These patches covered a total of 36,674 ha, with a median patch size of 37.7 ha and an interquartile range of 87.6 ha. Patches that burned in 2010 were not included as the fires may have burned after the lidar flight (June - August 2010).

To provide a comparison to post-burn structure, lidar metrics were also calculated for areas that were not disturbed for 1985–2010 according to the C2C Landsat record. Lidar metrics were averaged across each 1-km MODIS pixel using lidar cells that were not disturbed between 1985–2010 and that met the criteria in Section 2.3. MODIS pixels were analysed if they contained > 5 ha of suitable lidar cells. In total, structure was assessed for 15,642 undisturbed patches, with a median patch size of 14.6 ha and an interquartile range of 23.0 ha.

3. Results

Scatterplots between lidar metrics and productivity are displayed in Figure 3, with burned patches separated into five years since fire (YSF) groups. For comparison, the relationships for undisturbed patches (i.e., no disturbance detected for 1985–2010) are shown in the background of each panel.

Canopy cover (percent cover above 2m) was moderately related to GPP in patches with no record of disturbance between 1985–2010 ($r = 0.56$, $p < 0.001$). However, from 1–10 YSF, canopy cover was relatively low across all sampled productivities (mean = 13.3–16.0%), resulting in low variance between patches (sd = 8.4–8.9%) and weak correlations to GPP ($r = 0.18–0.34$). While canopy cover remained low in most patches at 11–15 YSF (mean = 11.0%, sd = 7.8%), canopy cover was moderately related to GPP at this time ($r = 0.48$, $p < 0.05$). By 16–20

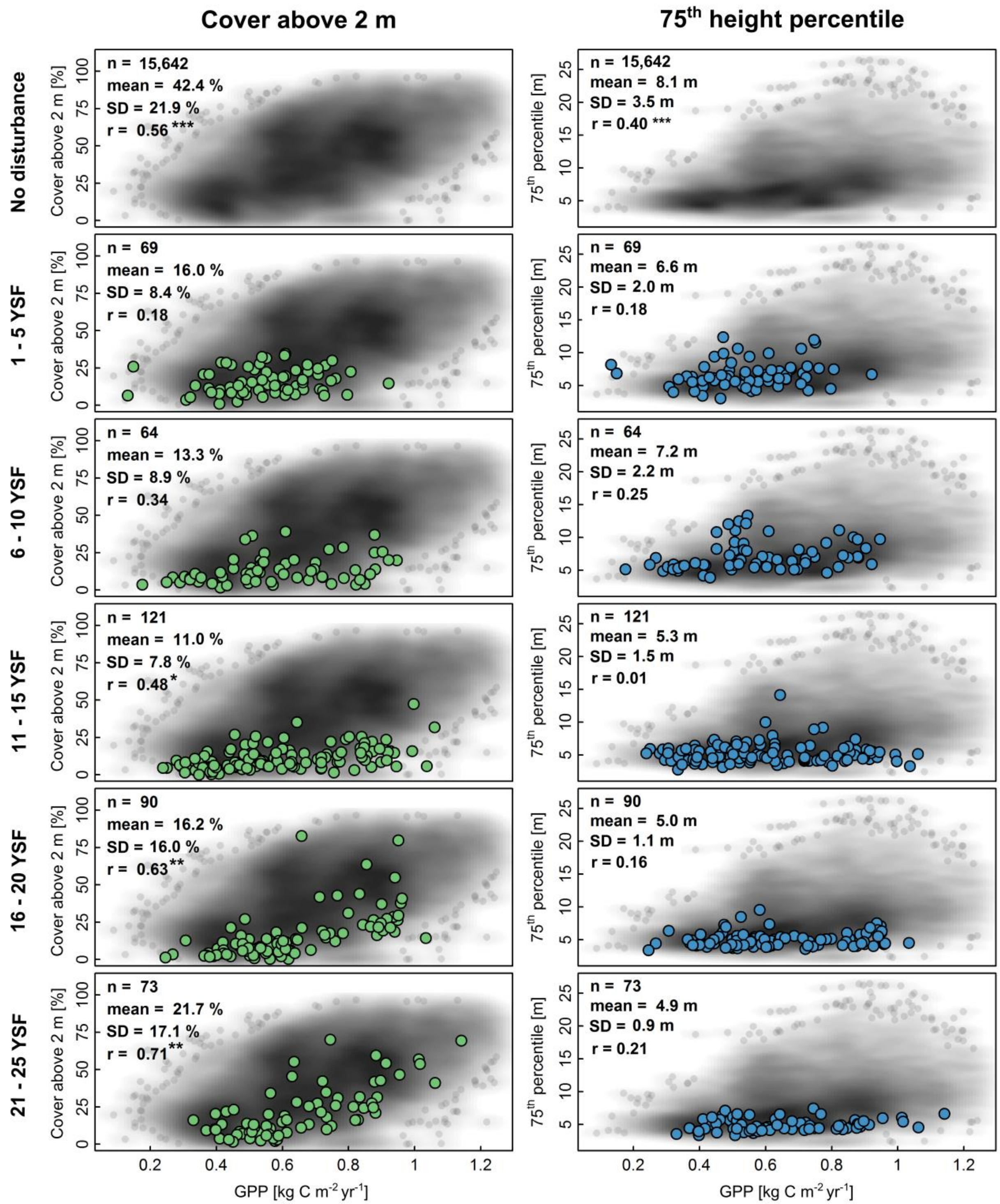

Figure 3: Scatterplots between lidar metrics and 2010 gross primary productivity (GPP) estimates for patches in five years since fire (YSF) groups. For comparison, patches that were undisturbed between 1985 – 2010 are displayed in the top panel, as well as in the background of subsequent panels. Summary statistics are provided for the lidar metrics. The significance of correlation coefficients were calculated using a distance interval of 20 km in the modified *t*-test (p< 0.05*, p < 0.01**, p < 0.001***). See Appendix S2 for information on the modified *t*-test.

YSF, a marked difference in canopy cover existed between patches with GPP < 0.7 $kgCm^{-2}yr^{-1}$ (mean = 9.1%) and patches with GPP > 0.7 $kgCm^{-2}yr^{-1}$ (mean = 29.5%), leading to an increase in variance (sd = 16.0 %) and a strong relationship to GPP ($r = 0.63$, $p < 0.01$). Canopy cover exceeded 40% in 8 of 90 patches at 16–20 YSF, while only one patch out of 254 exceeded 40% between 1–15 YSF. By 21–25 YSF, mean canopy cover increased to 21.7% and the correlation to GPP was strongest ($r = 0.71$, $p < 0.01$). At 21–25 YSF, canopy cover remained below 10% in more than half of low productivity patches (GPP < 0.6 $kgCm^{-2}yr^{-1}$), compared to only 5% of patches with GPP > 0.6 $kgCm^{-2}yr^{-1}$. The variability between patches at 16–20 YSF (sd = 16.0%) and 21–25 YSF (sd = 17.1%) was nearly has high as in undisturbed patches (sd = 21.9%).

The results of stand height (75^{th} height percentile) displayed a number of key differences to canopy cover (Figure 3). First, the correlation to GPP was weaker for stand height than canopy cover for undisturbed patches ($r = 0.40$, $p < 0.001$) and in all burned groups from 6–25 YSF ($r = 0.01$–0.25). While variance between patches increased for canopy cover from 11–15 YSF (sd = 7.8 %) to 21–25 YSF (sd = 17.1 %), variance decreased for stand height from 6–10 YSF (sd = 2.2 m) to 21–25 YSF (sd = 0.9 m). Mean stand height also decreased from 6–10 YSF (mean = 7.2 m) to 21–25 YSF (mean = 4.9 m), at which time stand height was low across all sampled productivities. While the relationship between canopy cover and GPP was stronger at 21–25 YSF than in undisturbed patches, the correlation between stand height and GPP remained weak and insignificant at 21–25 YSF ($r = 0.21$).

Figure 4a displays the relationship between canopy cover and stand height for burned patches as well as undisturbed patches. Canopy cover and stand height were strongly correlated in patches with no record of disturbance ($r = 0.79$, $p < 0.001$), but were weakly related in stands that burned between 1985–2009 ($r = 0.21$, $p < 0.05$). Patches at 1–10 YSF tended to be taller

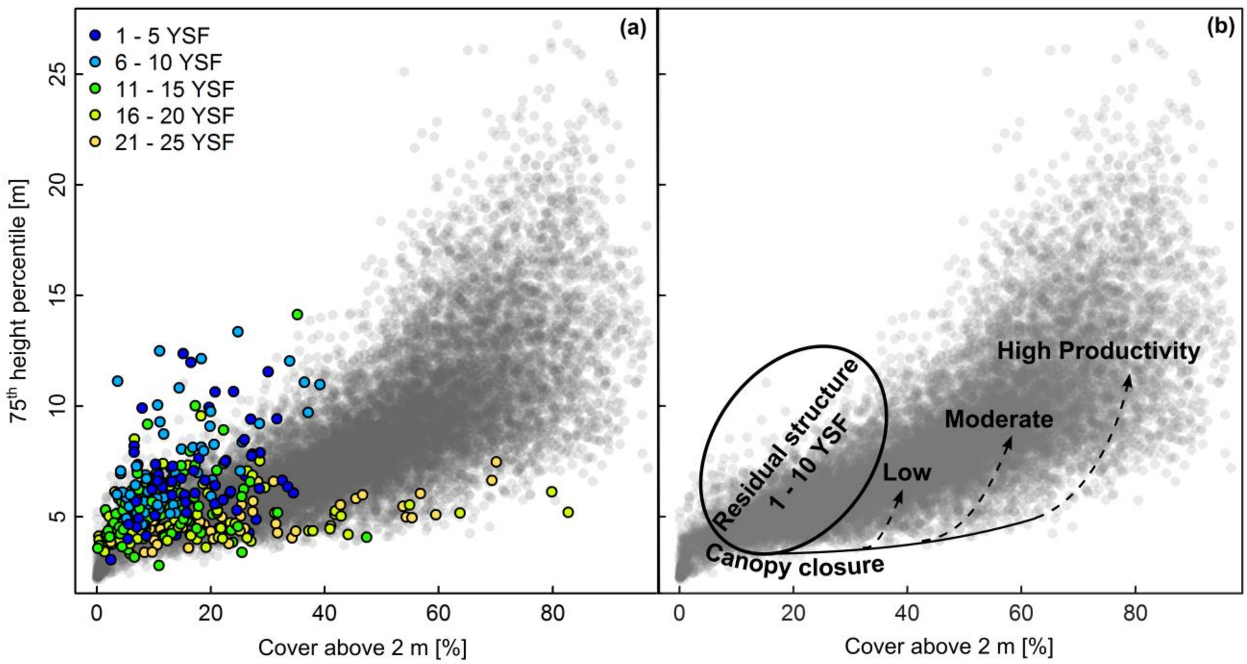

Figure 4: a) Relationship between lidar-derived estimates of canopy cover (cover above 2m) and stand height (75th percentile) for all burned patches, with points shaded according to years since fire (YSF). For comparison, all patches that had no record of disturbance between 1985 – 2010 are displayed in the background. b) Schematic interpretation of structural development following boreal fire, as assessed using lidar structural metrics. Dashed lines represented expected height gains after 25 YSF.

than undisturbed patches with similar canopy cover, and tall relative to burned patches from 11–25 YSF. For example, when canopy cover was low (< 40 %), stand heights > 7m were common between 1–10 YSF (37% of patches), but rare in other burned groups (6% of patches) and in undisturbed patches (7% of cells). In contrast, when canopy cover exceed 40% in burned patches, stands tended to be short relative to undisturbed patches with similar cover. The mean height for undisturbed patches was nearly double that of burned patches when canopy cover exceeded 40% (mean = 10.2m and 5.4m, respectively).

4. Discussion

Our results clearly demonstrate the influence of both time since fire and forest productivity on forest structure across the Canadian boreal. While estimates of canopy cover and stand height were related to satellite-derived estimates of GPP in stands with no record of disturbance (1985-2010), these same relationships did not exist in the first decade following fire, highlighting the stand replacing nature of the sampled fires (Mack *et al.*, 2008; de Groot *et al.*, 2013) and the slow establishment and growth of boreal trees (Johnstone *et al.*, 2004; Harper *et al.*, 2005; Bartels *et al.*, 2016). Specifically, low canopy cover estimates from 1 to 5 YSF imply that stands were relatively open regardless of forest productivity, as most tree cover was removed by fire. Canopy cover was below 10% in more than half of the patches at 11–15 YSF, as insufficient time had passed for new overstory canopies to form. At boreal sites in Alaska and the Yukon, Johnstone *et al.* (2004) found that trees typically took 3–7 years to establish after fire. This delayed establishment time, coupled with slow boreal growth rates, supports our finding that variability in canopy structure would not be observable along productivity gradients until at least the second decade after stand-replacing fire.

4.1. ***Variability in canopy cover increases as time since fire increases***

Following fire, the canopies of high productivity sites will begin to refill first, as favorable site conditions and longer growing seasons allow for faster growth (Bonan & Shugart, 1989; Johnstone *et al.*, 2004; Mack *et al.*, 2008). In addition to reaching canopy closure first, these canopies will also be the most densely vegetated, as competition for resources and poor growing conditions can limit the number of trees that establish and grow on lower productivity sites (Harper *et al.*, 2005; Johnstone & Chapin, 2006; Lecomte *et al.*, 2006). Between 16–25 YSF, estimates of canopy cover clearly captured this variability in the timing of canopy refilling and the density of regenerating canopies. In particular, variability in productivity had finally translated into structural differences by 16 – 20 YSF, as sufficient regeneration had occurred above 2 m in height in high productivity stands (GPP > 0.7 $kgCm^{-2}yr^{-1}$), while the canopies of lower productivity stands remained relatively open. Pioneer trees likely remained below 2 m in height by the end of the chronosequence in many of the lowest productivity patches (GPP < 0.6 $kgCm^{-2}yr^{-1}$), or few trees had established these sites, as canopy cover estimates remained below 10% in more than half of these low productivity patches at 21 – 25 YSF. However, canopy cover may have been below 10% in some patches in the analysis because trees never occupied the patch.

4.2. ***Stand height and canopy cover tell alternate stories of recovery***

While estimates of canopy cover captured the opening of forest canopies by fire and the slow formation of new canopies, estimates of stand height told a different story during the first 25 YSF. In the first decade after fire, stand height estimates were typically higher than expected from young, regenerating vegetation, suggesting the presence of residual structures (i.e., snags or surviving trees) in the canopy, similar to the findings of Kane *et al.* (2013) and Bolton *et al.* (2015). The height of residual structures was not related to productivity, as the characteristics of snags and surviving trees are primarily a function of fire severity, pre-disturbance structure, and stochastic processes that determine if trees survive and remain standing (e.g., Angers *et al.*, 2011). The transition from canopies dominated by snags and surviving trees to canopies dominated by regenerating trees was captured by the decrease in mean stand height from 6–10 YSF (7.2 m) to 21–25 YSF (4.9 m). While snags can persist for longer than 10 YSF, they no longer contribute significantly to the calculation of lidar metrics once canopies are dominated by pioneer trees, as these snags represent a smaller proportion of the vegetation above 2 m in height.

Rapid regeneration and vertical growth by broadleaf species may also contribute to the stand heights observed in the first 10 YSF. However, the absence of these tall stands later in the chronosequence, and the relatively low canopy cover estimates for these stands (Figure 4a), suggests that these early height estimates are from residual structures. In studies that use lidar-derived height metrics to assess post-fire regeneration, the presence of residual structures in the canopy must be considered, or the rate of regeneration could be overestimated.

While the number of trees that establish a site can vary widely between early successional stands, height differences between stands will be minimal in the first 25 YSF, as short growing seasons limit the rate of growth, and therefore, the range of heights of pioneer trees (Boucher *et al.*, 2006). This was confirmed by the low variability in stand height between patches from 16–25 YSF, as insufficient time had passed for differences in vertical growth to become pronounced along gradients of productivity. Alternatively, variability in canopy cover was nearly as high as in undisturbed stands by 16–25 YSF, as variability in tree establishment can be observed as soon as new canopies begin to form.

Patches that did show strong signs of tree regeneration in the first 25 YSF (i.e., high canopy cover) remained short-statured, suggesting discrepancies in carbon storage compared to undisturbed patches with similar canopy cover (Figure 4a). This has important implications for monitoring recovery with optically sensed data, as optical measures of vegetation are more sensitive to canopy infilling than vertical growth (Goetz & Dubayah, 2011). Specifically, while optical indices may return to pre-disturbance values once canopies reach crown closure, large differences in the vertical structure of stands will remain. Therefore, both horizontal and vertical components of forest recovery should be assessed when aiming to characterize carbon uptake by forests (Frolking *et al.*, 2009).

Following stand replacing disturbance, Pickell *et al.* (2016) demonstrated how rapidly some Landsat vegetation indices return to pre-disturbance conditions from samples across the Canadian boreal. For instance, when applying the normalized difference vegetation index (NDVI), Pickell *et al.* (2016) found that 93.4% of disturbed pixels recovered within five years (i.e., pixels reached at least 80% of pre-disturbance NDVI). Similar results were found using the normalized burn ratio (77.9% of pixels recovered in 5 years). At a coarser spatial-resolution, Hicke *et al.* (2003) found that Net Primary Productivity (NPP) returned to pre-disturbance values in approximately 9 years after fire in the boreal using 8-km estimates of NPP from the Advanced Very High Resolution Radiometer (AVHRR). These optical measures of recovery and productivity provide valuable information on the re-establishment of vegetation on burned sites, but alone cannot explain how recovery and productivity are realized in terms of canopy structure and aboveground biomass. By linking spectral trajectories to actual measurements of post-fire structure from lidar, an improved understanding of the information provided by satellite-derived estimates of recovery and productivity can be gained.

By bringing together the trends observed for canopy cover and stand height, we can build a schematic model of forest regeneration following boreal fire (Figure 4b). In the first decade following fire, canopy cover will likely be low regardless of productivity, while stand height estimates will vary depending on fire severity, pre-disturbance structure, and the stochastic processes that influence the characteristics of residual structures. Our results suggest that canopies will first fill in laterally prior to making significant gains in height, as the available growing space is re-occupied by pioneer trees. Once the growing space is filled, stands will continue to make vertical gains in height, and differences in height will likely become apparent across gradients of productivity. Due to the short chronosequence in this analysis, and the slow boreal growth rates, these increases in height were not observed. However, the large differences that exist between the height of stands at 21–25 YSF and stands with similar canopy cover, but no record of disturbance, suggest that significant vertical gains will be made in high productivity stands.

4.3. ***Considerations for interpreting results***

4.3.1. *The influence of averaging across burned patches*

Structural attributes were averaged across burned patches in this study, as the goal was to observe how post-fire structure and regeneration vary regionally, not locally, along gradients of productivity. Differences in fire severity, species composition, and site conditions likely existed within many of the sampled burned patches, leading to within-patch variability in forest regeneration (Johnstone *et al.*, 2004; Harper *et al.*, 2005; Lecomte *et al.*, 2006).. While substantial regeneration above 2-m was not observed across entire patches to signal regeneration until 16 – 20 YSF, tree regeneration could occur earlier at the sub-patch level on sites rapidly colonized by broadleaf species, or on high productivity sites colonized by coniferous species (Johnstone *et al.*, 2004; Bartels *et al.*, 2016). Averaging across patches also has important implications on the assessment of stand height variability. Differences in height would be expected between rapidly established broadleaf trees and slow growing conifers early after fire; however, averaging to the patch level appears to have masked these differences. While understanding fine-scale variability in forest regeneration is critical for many applications, our results provide important insights into how average post-fire conditions vary regionally, as this information is important for characterizing regional variations in carbon uptake following disturbance (Kurz *et al.*, 2013).

4.3.2. *Confusing residual structure and stand regeneration*

Further, determining the precise timing of residual structure loss and replacement by pioneer trees is difficult with lidar metrics, as these processes are gradual and occur simultaneously. The length of time that snags remain standing in boreal stands also varies widely (Boulanger & Sirois, 2006; Angers *et al.*, 2011). For black spruce stands in Quebec, for example, Boulanger and Sirois (2006) reported a half-life of 16.2 years (i.e., length of time for half of the snags to fall after mortality), while Angers *et al.* (2011) reported a half-life of only 4.4 years. By 11–15 YSF, when mean canopy cover was lowest, canopies may have been transitioning from residual structure dominance to dominance by pioneer trees. However, the amount of regeneration (i.e., increase in canopy cover) did not appear to outweigh the loss of residual structure (i.e., decrease in canopy cover), preventing clear evidence of regeneration from being observed for this group.

4.3.3. *MODIS GPP is inherently related to vegetation cover*

A final consideration for interpreting the results of this analysis involves the use of satellite-derived estimates of GPP to assess differences in forest productivity. As vegetation greenness (i.e., as related to the calculation of MODIS FPAR) is an important input to the MODIS GPP algorithm, GPP is inherently related to vegetation cover. Therefore, the strong correlations between MODIS GPP and canopy cover do not necessarily imply causation (i.e., high productivity sites can support denser canopies, but denser canopies can also lead to higher estimates of GPP). While a relationship between canopy cover and satellite GPP is therefore expected based on the inputs to the GPP algorithm, our results provide important insights into how these relationships vary through time, and how these satellite-derives estimates of productivity are realized structurally. Additionally, as a single 1-km MODIS cell covers 100 ha, and the median burned patch size was 37.7 ha, these GPP estimates serve more as an indicator of landscape productivity, as opposed to a precise measure of productivity within each burned patch.

5. Conclusions

By combining measures of structure from lidar with disturbance history from Landsat, variability in early stand succession can be characterized over large forested areas (Kane *et al.*, 2013, 2014; Bolton *et al.*, 2015). Our results highlight the need for spatially explicit characterizations of carbon uptake following fire across the boreal, as canopy structure varied strongly along gradients of productivity, but only after 15 YSF. The contrasting trends observed between canopy cover and stand height estimates in this analysis point to the need to monitor multiple aspects of forest recovery. Our findings suggest that estimates of canopy cover capture most of the variability in forest regeneration between early successional patches. However, if only canopy cover estimates are assessed, assumptions concerning the nature of forest recovery once canopy closure is reached can obscure the fact that large differences in stand height and carbon storage remain. Our results demonstrate the value of coarse-resolution estimates of productivity for describing regional variability in forest regeneration and carbon uptake following disturbance, which is of particular importance in unmanaged boreal forests, where limited inventory data is available to inform carbon modelling activities and disturbance rates are high (Gillis *et al.*, 2005; Kurz *et al.*, 2013). We expect that differences in canopy structure would be realized sooner along gradients of productivity in faster growing temperate and tropical ecosystems, and differences in both height and cover would be observable. As the length of the Landsat data record continues to increase, future studies can monitor later stages of forest succession using this approach, allowing for a more detailed understanding of the relationship between disturbance, productivity, and forest structure.

Acknowledgements

Components of this research were funded by a NSERC Discovery grant to Nicholas Coops and a graduate fellowship to Douglas Bolton. Chris Hopkinson (with the University of Lethbridge) is thanked for his transect project partnership, which was critical in obtaining the research data used in this study. Components of this research was undertaken as part of the "National Terrestrial Ecosystem Monitoring System (NTEMS): Timely and detailed national cross-sector monitoring for Canada" project jointly funded by the Canadian Space Agency (CSA) Government Related Initiatives Program (GRIP) and the Canadian Forest Service (CFS) of Natural Resources Canada. Christopher Bater (Government of Alberta) is thanked for his analysis efforts and insights into the processing of the lidar transects. Trevor Milne of Gaiamatics is thanked for assisting with the development of customized code for processing the lidar transects.

References

Amiro, B.D., Stocks, B.J., Alexander, M.E., Flannigan, M.D. & Wotton, B.M. (2001) Fire, climate change, carbon and fuel management in the Canadian boreal forest. *International Journal of Wildland Fire*, **10**, 405–413.

Andrew, M.E., Wulder, M.A. & Coops, N.C. (2012) Identification of de facto protected areas in boreal Canada. *Biological Conservation*, **146**, 97–107.

Angers, V.A., Gauthier, S., Drapeau, P., Jayen, K. & Bergeron, Y. (2011) Tree mortality and snag dynamics in North American boreal tree species after a wildfire: a long-term study. *International Journal of Wildland Fire*, **20**, 751–763.

Bartels, S.F., Chen, H.Y.H., Wulder, M.A. & White, J.C. (2016) Trends in post-disturbance recovery rates of Canada's forests following wildfire and harvest. *Forest Ecology and Management*, **361**, 194–207.

Bolton, D.K., Coops, N.C. & Wulder, M.A. (2013) Measuring forest structure along productivity gradients in the Canadian boreal with small-footprint Lidar. *Environmental Monitoring and Assessment*, **185**, 6617–34.

Bolton, D.K., Coops, N.C. & Wulder, M.A. (2015) Characterizing residual structure and forest recovery following high-severity fire in the western boreal of Canada using Landsat time-series and airborne lidar data. *Remote Sensing of Environment*, **163**, 48–60.

Bonan, G.B. & Shugart, H.H. (1989) Environmental factors and ecological processes in boreal forests. *Annual Review of Ecology and Systematics*, **20**, 1–28.

Boucher, D., Gauthier, S. & De Grandpré, L. (2006) Structural changes in coniferous stands along a chronosequence and a productivity gradient in the northeastern boreal forest of Québec. *Ecoscience*, **13**, 172–180.

Boulanger, Y. & Sirois, L. (2006) Postfire dynamics of black spruce coarse woody debris in northern boreal forest of Quebec. *Canadian Journal of Forest Research*, **36**, 1770–1780.

Brandt, J.P., Flannigan, M.D., Maynard, D.G., Thompson, I.D. & Volney, W.J.A. (2013) An introduction to Canada's boreal zone: ecosystem processes, health, sustainability, and environmental issues. *Environmental Reviews*, **21**, 207–226.

Brandt, J.P.P. (2009) The extent of the North American boreal zone. *Environmental Reviews*, **17**, 101–161.

Brassard, B.W. & Chen, H.Y.H. (2006) Stand structural dynamics of North American boreal forests. *Critical Reviews in Plant Sciences*, **25**, 115–137.

Chen, H.Y.H. & Popadiouk, R. V (2002) Dynamics of North American boreal mixedwoods. *Environmental Reviews*, **10**, 137–166.

Clifford, P., Richardson, S. & Hémon, D. (1989) Assessing the significance of the correlation between two spatial processes. *Biometrics*, **45**, 123–134.

Dutilleul, P., Clifford, P., Richardson, S. & Hemon, D. (1993) Modifying the t test for assessing the correlation between two spatial processes. *Biometrics*, **49**, 305–314.

Ecological Stratification Working Group (1996) *A National Ecological Framework for Canada.* Centre for Land and Biological Resources Research, Research Branch, Agriculture and Agri-Food Canada, Ottawa, ON, Canada.

Fluet-Chouinard, E., Lehner, B., Rebelo, L.-M., Papa, F. & Hamilton, S.K. (2015) Development of a global inundation map at high spatial resolution from topographic downscaling of coarse-scale remote sensing data. *Remote Sensing of Environment*, **158**, 348–361.

Frolking, S., Palace, M.W., Clark, D.B., Chambers, J.Q., Shugart, H.H. & Hurtt, G.C. (2009) Forest disturbance and recovery: A general review in the context of spaceborne remote sensing of impacts on aboveground biomass and canopy structure. *Journal of Geophysical Research*, **114**, 1–27.

Gillis, M.D., Omule, A.Y. & Brierley, T. (2005) Monitoring Canada's forests: the National Forest Inventory. *The Forestry Chronicle*, **81**, 214–221.

Goetz, S. & Dubayah, R. (2011) Advances in remote sensing technology and implications for measuring and monitoring forest carbon stocks and change. *Carbon Management*, **2**, 231–244.

de Groot, W.J., Cantin, A.S., Flannigan, M.D., Soja, A.J., Gowman, L.M. & Newbery, A. (2013) Forest Ecology and Management A comparison of Canadian and Russian boreal forest fire regimes. *Forest Ecology and Management*, **294**, 23–34.

Hansen, M.C. & Loveland, T.R. (2012) A review of large area monitoring of land cover change using Landsat data. *Remote Sensing of Environment*, **122**, 66–74.

Harper, K.A., Bergeron, Y., Drapeau, P., Gauthier, S. & De Grandpré, L. (2005) Structural development following fire in black spruce boreal forest. *Forest Ecology and Management*, **206**, 293–306.

Harper, K.A., Bergeron, Y., Gauthier, S. & Drapeau, P. (2002) Post-Fire Development of Canopy Structure and Composition in Black Spruce Forests of Abitibi , Québec : A Landscape Scale Study. *Silva Fennica*, **36**, 249 – 263.

Hermosilla, T., Wulder, M.A., White, J.C., Coops, N.C., Hobart, G.W. & Campbell, L.B. (2016) Mass data processing of time series Landsat imagery: pixels to data products for forest monitoring. *International Journal of Digital Earth*, **9**, 1035–1054.

Hicke, J.A., Asner, G.P., Kasischke, E.S., French, N.H.F., Randerson, J.T., Collatz, G.J., Stocks, B.J., Tucker, C.J., Los, S.O. & Field, C.B. (2003) Postfire response of North American boreal forest net primary productivity analyzed with satellite observations. *Global Change Biology*, **9**, 1145–1157.

Huang, C., Goward, S.N., Masek, J.G., Thomas, N., Zhu, Z. & Vogelmann, J.E. (2010) An automated approach for reconstructing recent forest disturbance history using dense Landsat time series stacks. *Remote Sensing of Environment*, **114**, 183–198.

Jennings, S.B., Brown, N.D. & Sheil, D. (1999) Assessing forest canopies and understorey illumination: canopy closure, canopy cover and other measures. *Forestry*, **72**, 59–73.

Johnstone, J.F., Chapin III, F.S., Foote, J., Kemmett, S., Price, K. & Viereck, L. (2004) Decadal observations of tree regeneration following fire in boreal forests. *Canadian Journal of Forest Research*, **34**, 267–273.

Johnstone, J.F. & Chapin, F.S. (2006) Effects of soil burn severity on post-fire tree recruitment in boreal forest. *Ecosystems*, **9**, 14–31.

Kane, V.R., Lutz, J.A., Roberts, S.L., Smith, D.F., McGaughey, R.J., Povak, N.A. & Brooks, M.L. (2013) Landscape-scale effects of fire severity on mixed-conifer and red fir forest structure in Yosemite National Park. *Forest Ecology and Management*, **287**, 17–31.

Kane, V.R., North, M.P., Lutz, J.A., Churchill, D.J., Roberts, S.L., Smith, D.F., McGaughey, R.J., Kane, J.T. & Brooks, M.L. (2014) Assessing fire effects on forest spatial structure using a fusion of Landsat and airborne LiDAR data in Yosemite National Park. *Remote Sensing of Environment*, **151**, 89–101.

Kasischke, E.S., Christensen, N.L. & Stocks, B.J. (1995) Fire , global warming , and the carbon balance of boreal forests. *Ecological Applications*, **5**, 437–451.

Kennedy, R.E., Yang, Z. & Cohen, W.B. (2010) Detecting trends in forest disturbance and recovery using yearly Landsat time series : 1 . LandTrendr — Temporal segmentation algorithms. *Remote Sensing of Environment*, **114**, 2897–2910.

Kurz, W.A., Shaw, C.H., Boisvenue, C., Stinson, G., Metsaranta, J., Leckie, D., Dyk, A., Smyth, C. & Neilson, E.T. (2013) Carbon in Canada ' s boreal forest — A synthesis. *Environmental Reviews*, **21**, 260–292.

Larson, A.J., Lutz, J.A., Gersonde, R.F., Franklin, J.F. & Hietpasi, F.F. (2008) Potential site productivity influences the rate of forest structural development. *Ecological Applications*, **18**, 899–910.

Lecomte, N., Simard, M., Fenton, N. & Bergeron, Y. (2006) Fire severity and long-term ecosystem biomass dynamics in coniferous boreal forests of eastern Canada. *Ecosystems*, **9**, 1215–1230.

Lefsky, M.A., Turner, D.P., Guzy, M. & Cohen, W.B. (2005) Combining lidar estimates of aboveground biomass and Landsat estimates of stand age for spatially extensive validation of modeled forest productivity. *Remote Sensing of Environment*, **95**, 549–558.

Lim, K., Treitz, P., Wulder, M.A., St-Onge, B. & Flood, M. (2003) LiDAR remote sensing of forest structure. *Progress in Physical Geography*, **27**, 88–106.

Mack, M.C., Treseder, K.K., Manies, K.L., Harden, J.W., Schuur, E. a. G., Vogel, J.G., Randerson, J.T. & Chapin, F.S. (2008) Recovery of Aboveground Plant Biomass and Productivity After Fire in Mesic and Dry Black Spruce Forests of Interior Alaska. *Ecosystems*, **11**, 209–225.

Magnussen, S. & Wulder, M.A. (2012) Post-fire canopy height recovery in Canada's boreal forests using Airborne Laser Scanner (ALS). *Remote Sensing*, **4**, 1600–1616.

Næsset, E., Gobakken, T., Holmgren, J., Hyyppa, H., Hyyppa, J., Maltamo, M., Nilsson, M., Olsson, H., Persson, A. & Soderman, U. (2004) Laser scanning of forest resources: the Nordic experience. *Scandinavian Journal of Forest Research*, **19**, 482–499.

Pan, Y., Birdsey, R.A., Fang, J., Houghton, R., Kauppi, R.E., Kurz, W.A., Phillips, O.L., Shvidenko, A., Lewis, S.L., Canadell, J.G., Ciais, P., Jackson, R.B., Pacala, S.W., McGuire, A.D., Piao, S., Rautiainen, A., Sitch, S. & Hayes, D. (2011) A large and persistent carbon sink in the world's forests. *Science*, **333**, 988–993.

Pare, D. & Bergeron, Y. (1995) Above-ground biomass accumulation along a 230-year chronosequence in the southern portion of the Canadian boreal forest. *Journal of Ecology*, **83**, 1001–1007.

Pickell, P.D., Hermosilla, T., J. Frazier, R., Coops, N.C. & Wulder, M.A. (2016) Forest recovery trends derived from Landsat time series for North American boreal forests. *International Journal of Remote Sensing*, **37**, 138–149.

Running, S.W., Nemani, R., Heinsch, F.A., Zhao, M., Reeves, M. & Hashimoto, H. (2004) A continuous satellite-derived measure of global terrestrial primary production. *BioScience*, **54**, 547–560.

Ryan, K.C. (2002) Dynamic Interactions between Forest Structure and Fire Behavior in Boreal Ecosystems. *Silva Fennica*, **36**, 13–39.

Venier, L.A., Thompson, I.D., Fleming, R., Malcolm, J., Aubin, I., Trofymow, J.A., Langor, D., Sturrock, R., Patry, C., Outerbridge, R.O., Holmes, S.B., Haeussler, S., Grandpré, L. De, Chen, H.Y.H., Bayne, E., Arsenault, A. & Brandt, J.P. (2014) Effects of natural resource development on the terrestrial biodiversity of Canadian boreal forests. *Environmental Reviews*, **22**, 457–490.

Wulder, M.A., Masek, J.G., Cohen, W.B., Loveland, T.R. & Woodcock, C.E. (2012a) Opening the archive: How free data has enabled the science and monitoring promise of Landsat. *Remote Sensing of Environment*, **122**, 2–10.

Wulder, M.A., White, J.C., Bater, C.W., Coops, N.C., Hopkinson, C. & Chen, G. (2012b) Lidar plots — a new large-area data collection option: context, concepts, and case study. *Canadian Journal of Remote Sensing*, **38**, 600–618.

Wulder, M.A., White, J.C., Cranny, M., Hall, R.J., Luther, J.E., Beaudoin, A., Goodenough, D.G. & Dechka, J.A. (2008) Monitoring Canada's forests. Part 1: Completion of the EOSD land cover project. *Canadian Journal of Remote Sensing*, **34**, 549–562.

SUPPORTING INFORMATION

Assessing variability in post-fire forest structure along gradients of productivity in the Canadian boreal using multi-source remote sensing

Douglas K. Bolton, Nicholas C. Coops, Txomin Hermosilla, Michael A. Wulder, Joanne C. White

Appendix S1: Data specifications and preprocessing

Appendix S2: The modified *t*-test for correlation

Appendix S1: Data specifications and preprocessing

Lidar structural measurements

The 34 transects of lidar data were collected between June and August of 2010 by the Canadian Forest Service in collaboration with the Consortium for Lidar Environmental Applications Research (C-CLEAR) and the Applied Geomatics Research Group (Wulder et al., 2012). The data were collected by an Optech ALTM 3100 discrete return sensor, which had a fixed scan angle of 15° and a pulse repetition frequency of 70 kHz. The transects were flown between the altitudes of 1200 – 1900 m, had a minimum swath width of 400 m, an average return density of 2.8 returns/m^2, and totaled approximately 25,000 km in length. The average transect length, which was largely determined by the location of suitable airports, was approximately 700 km (Hopkinson et al., 2011).

These lidar data were preprocessed using customized software designed to handle large transect files, which included the classification lidar returns into ground and non-ground (Hopkinson et al., 2011). The data were divided into 25- by 25-m cells and lidar metrics describing the density and distribution of returns were calculated for each cell in the FUSION software package (available at: http://forsys.cfr.washington.edu/fusion/fusionlatest.html, see Wulder et al., 2012 for a full list of calculated metrics). From the over 18 billion lidar returns collected, lidar metrics were generated for more than 17 million 25 by 25-m cells.

Lidar cells were removed if they contained fewer than 0.5 returns/m^2. Cells with a 75^{th} height percentile greater 50 m were masked from the analysis, as these height estimates were likely erroneous due to steep terrain or atmospheric anomalies (< 0.01% of cells had a 75^{th} height percentile > 50 m).

Landsat disturbance detection

The Composite 2 Change (C2C) approach, developed by Hermosilla et al. (2016), was used to identify burned patches across the entire boreal of Canada. Following the C2C approach, best-available pixel (BAP) image composites were first produced from Landsat imagery by selecting the best observations for each pixel within a specific date range (August 1 +/- 30 days) based on the scoring functions defined by White et al. (2014), which rank the presence and distance to clouds and their shadows, the atmospheric quality, and the acquisition sensor. Next, these image composites were further refined by removing noisy observations (e.g., haze and smoke) and infilling data gaps using spectral trend analysis of pixel time series (Hermosilla et al., 2015a). This step results in the production of seamless annual surface reflectance composites for all of Canada from 1984 to 2012, as well as the detection and characterization of forest change events. The overall detection accuracy for change events was 89.0%, with 89.3% of change events detected in the correct year, and 97.7% detected within ±1 year. Following the object-based image analysis approach introduced in Hermosilla et al. (2015b), the changes detected were attributed to a change type (i.e., fire, harvesting, road, or non-stand-replacing), based on their spectral, temporal, and geometrical characteristics using a Random Forests classifier, with an overall accuracy of 92%. Fire detection had the highest producer's (93%) and user's (98%) accuracy.

MODIS gross primary productivity

The MODIS gross primary productivity (GPP) algorithm provides 8-day estimates of GPP globally at 1-km spatial resolution. Derived following the principles of Monteith (1972), GPP is determined for each 1-km cell as a function of the absorbed photosynthetically active radiation (APAR) and the light-use efficiency (LUE) of vegetation:

$$GPP = \varepsilon max * 0.45 * SWrad * FPAR * fVPD * fTmin$$

where εmax is the maximum LUE; SWrad is the incoming short-wave solar radiation; which is multiplied by 0.45 to derive photosynthetically active radiation (PAR); FPAR is the fraction of incident PAR that is absorbed by vegetation; and fVPD and fTmin are modifiers which reduce GPP when vapor pressure deficit (VPD) or temperature limit plant function (Zhao and Running 2010).

Within the algorithm, εmax is varied based on vegetation type, which is determined using the MODIS Land Cover Type product (MOD12Q1) (Friedl et al., 2010). Minimum daily temperature (Tmin), VPD, and SWrad are calculated from daily meteorological data, while FPAR is determined using the 1-km MODIS FPAR product (MOD15A2) (Myneni et al., 2011), which is computed from MODIS surface reflectance values (Zhao & Running, 2010).

Heinsch et al. (2006) found that annual GPP estimates from MODIS correlated strongly to annual flux tower estimates of GPP across North America ($r = 0.859 \pm 0.173$), but predicted higher GPP than tower estimates at most sites (relative error = 24%).

We obtained a re-processed version of MOD17A3, which addresses cloud and aerosol contamination issues (Zhao & Running, 2010, available at: http://www.ntsg.umt.edu/project/mod17). As vegetation type is an important input to the

GPP algorithm and can significantly influence GPP (Running et al., 2004), only cells classified as forest (i.e., > 10% tree cover according to the class definition) or shrubland in the 2010 MODIS Land Cover Type product were included in the analysis (Classes 1 to 9 according to the University of Maryland classification scheme).

Appendix S2: The modified *t*-test for correlation

The modified *t*-test, introduced by Clifford et al. (1989) and modified by Dutilleul (1993), was used to assess the significance of the correlations between structural attributes and GPP. When data is spatially autocorrelated, standard *t*-tests are not valid for testing the significance of a correlation, as each sample does not represent a full degree of freedom (Clifford et al., 1989). In the modified *t*-test, the degrees of freedom are reduced through the calculation of an "effective sample size", which is inversely proportion to the amount of spatial autocorrelation in each variable (see Dutilleul 1993). To calculate the effective sample size, the distances between all pairs of points are divided into *k* distance strata and spatial autocorrelation is assessed for both variables of interest. The selection of *k* impacts the calculation of the effective sample size, as larger values of *k* (i.e., shorter distance interval) will result in a higher calculated spatial autocorrelation and, therefore, a lower effective sample size (Fortin & Payette, 2002). Fortin and Payette (2002) varied *k* between 5 and 15 in a study of boreal fire events (distance interval = 20–60 km), and found that while the effective sample size did change, varying *k* did not affect the rejection of their null hypothesis. To assess the sensitivity of our results to the selection of *k*, three distance intervals were tested: 10, 20, and 40 km. The modified *t*-test was calculated using the Dutilleul (1993) modification in Pattern Analysis, Spatial Statistics and Geographic Exiegesis (PASSaGE; Rosenberg and Anderson 2011).

As the modified *t*-test is computationally intensive, 2000 patches were randomly sampled for the undisturbed group to test the significance of the relationship between lidar metrics and productivity.

Varying the distance interval from 10 km to 40 km in the modified t-test did not change the significance of any correlation coefficients (α = 0.05), however, the level of significance did change from $p < 0.05$ to $p < 0.01$ in several cases. Results in the main text were produced using a distance interval of 20 km.

References

Clifford, P., Richardson, S. & Hémon, D. (1989) Assessing the significance of the correlation between two spatial processes. *Biometrics*, **45**, 123–134.

Dutilleul, P. (1993) Modifying the t test for assessing the correlation between two spatial processes. *Biometrics*, **49**, 305–314.

Fortin, M. & Payette, S. (2002) How to test the significance of the relation between spatially autocorrelated data at the landscape scale : A case study using fire and forest maps. *Ecoscience*, **9**, 213–218.

Friedl, M.A., Sulla-Menashe, D., Tan, B., Schneider, A., Ramankutty, N., Sibley, A. & Huang, X. (2010) MODIS Collection 5 global land cover: Algorithm refinements and characterization of new datasets. *Remote Sensing of Environment*, **114**, 168–182.

Heinsch, F.A., Running, S.W., Kimball, J.S., Nemani, R.R., Davis, K.J., Bolstad, P. V, Cook, B.D., Desai, A.R., Ricciuto, D.M., Law, B.E., Oechel, W.C., Wofsy, S.C., Dunn, A.L., Munger, J.W., Baldocchi, D.D., Hollinger, D.Y., Richardson, A.D., Stoy, P.C., Siqueira, M.B.S., Monson, R.K., Burns, S.P. & Flanagan, L.B. (2006) Evaluation of remote sensing based terrestrial productivity from MODIS using regional tower eddy flux network observations. *IEEE Transactions on Geoscience and Remote Sensing*, **44**, 1908–1925.

Hermosilla, T., Wulder, M., White, J.C., Coops, N. & Hobart, G.W. (2015a) An integrated Landsat time series protocol for change detection and generation of annual gap-free surface reflectance composites. *Remote Sensing of Environment*, **158**, 220–234.

Hermosilla, T., Wulder, M.A., White, J.C., Coops, N.C. & Hobart, G.W. (2015b) Regional detection, characterization, and attribution of annual forest change from 1984 to 2012 using Landsat-derived time-series metrics. *Remote Sensing of Environment*,

170, 121–132.
Hermosilla, T., Wulder, M.A., White, J.C., Coops, N.C., Hobart, G.W. & Campbell, L.B. (2016) Mass data processing of time series Landsat imagery: pixels to data products for forest monitoring. *International Journal of Digital Earth*, **9**, 1035–1054.
Hopkinson, C., Wulder, M.A., Coops, N.C., Milne, T., Fox, A. & Bater, C.W. (2011) Airborne lidar sampling of the Canadian boreal forest: Planning, execution, and initial processing. *Proceedings of the SilviLaser 2011 Conference*, Hobart, Australia.
Monteith, J.L. (1972) Solar radiation and productivity in tropical ecosystems. *Journal of Applied Ecology*, **9**, 747–766.
Myneni, R., Knyazikhin, Y. & Shabanov, N. (2011) Leaf area index and fraction of absorbed PAR products from Terra and Aqua MODIS sensors: analysis, validation, and refinement. *Land remote sensing and global environmental change* (ed. by B. Ramachandran, C.O. Justice, and M.J. Abrams), pp. 603–633. Springer, New York.
Running, S.W., Nemani, R., Heinsch, F.A., Zhao, M., Reeves, M. & Hashimoto, H. (2004) A continuous satellite-derived measure of global terrestrial primary production. *BioScience*, **54**, 547–560.
White, J.C., Wulder, M.A., Hobart, G.W., Luther, J.E., Hermosilla, T., Griffiths, P., Coops, N.C., Hall, R.J., Hostert, P., Dyk, A. & Guindon, L. (2014) Pixel-based image compositing for large-area dense time series applications and science. *Canadian Journal of Remote Sensing*, **40**, 192–212.
Wulder, M.A., White, J.C., Bater, C.W., Coops, N.C., Hopkinson, C. & Chen, G. (2012) Lidar plots — a new large-area data collection option: context, concepts, and case study. *Canadian Journal of Remote Sensing*, **38**, 600–618.
Zhao, M. & Running, S.W. (2010) Drought-induced reduction in global terrestrial net primary production from 2000 through 2009. *Science*, **329**, 940–943.